R_{sh}/Q_0 Measurements in Klystron Cavities

Robson K. B. e Silva
Navy Technology Center at Sao Paulo
CTMSP
Av. Prof. Lineu Prestes, 2468
São Paulo, SP, Brazil
rkeller@usp.br

Daniel T.Lopes
Nuclear and Energy Research Institute
IPEN
Av. Prof. Lineu Prestes, 2242
São Paulo, SP, Brazil
danieltl@usp.br

Cláudio C. Motta
University of Sao Paulo
USP
Av. Prof. Lineu Prestes, 2468
São Paulo, SP, Brazil
ccmotta@usp.br

Abstract—**This paper presents the experimental results of R_{sh}/Q_0 measurements in klystron cavities using the perturbation technique. The theory involving this technique results in an expression which depends on the natural frequency f_0 and the perturbed frequency shift Δf, both measured using a cylindrical reentrant cavity with offset gap built in the laboratory. In addition, it is used a cylindrical cavity (pill-box) to calculate a constant that depends on the geometry of the perturbed object, as well as analytical expressions to calculate an integral factor that relates the square of the voltage on axis and the electric energy originally stored in the small volume of the perturbed object. The values measured of f_0, Δf and R_{sh}/Q_0 are, respectively, 2.86 GHz, - 5.27 MHz and 79.8 Ω. They are also compared with the results simulated by a 3D eigensolver obtaining a good agreement.**

Keywords – Klystron cavity R_{sh}/Q_0, Slater's perturbation technique, cylindrical reentrant cavity, perturbed frequency shift.

I. INTRODUCTION

The cavity R_{sh}/Q_0 is one of the most important parameters to be determined in the design of a klystron amplifier. In this problem the gain of a klystron is proportional to the cavity shunt resistance R_{sh}, while bandwidth proportional to the cavity $1/Q_0$, so that R_{sh}/Q_0 is a useful figure of merit in describing the effect of the each cavity on the gain-bandwidth product of overall amplifier. Therefore, it is relevant when, for example, one of the design requirements is high product gain-bandwidth. Moreover, since the R_{sh}/Q_0 quantity is independent of cavity losses it is a very relevant figure of merit. Furthermore, it is dependent on the geometric shape of the cavity and frequency.

Although there are some electromagnetic field codes available now to calculate of the cavity R_{sh}/Q_0, the experimental measurements provide considerable insight on the role of a cavity and its gap [1]-[3] over the amplifier. Accordingly to Slater's perturbation theorem [4], when some parameters such as the configuration of the boundary, the material in the volume or the material of the boundary change slightly, the electromagnetic system is said to be perturbed. If the solution of an unperturbed problem is known, then the solution of the perturbed problem, which is slightly different from the unperturbed one, can be obtained by means of the principle of the perturbation. There are two possible ways to do this: the cavity wall perturbation or the conductor perturbation of the cavity. The first one means to introduce a small deformation in the wall. The second one means to introduce a small conductive perturbing object into the cavity. In this work the latter technique is used, although the deformation of the wall may also be considered as a conductive perturbing object stuck on the wall.

Given a cavity at resonance, it is known that average stored magnetic and electric energies are equals. If a small perturbation is made by introducing a small conductive object into the cavity, this changes one type of energy more than the other, and resonant frequency would then shift by an amount necessary to equalize the energies again. The perturbation method assumes that the actual fields of a cavity with a small shape or material perturbation are not different from those of the unperturbed cavity. So, if the cavity frequency shift due to the small object can be measured as well its geometry shape, the Slater's perturbation theorem is useful to determine the cavity figure of merit R_{sh}/Q_0.

This paper is organized as follows. Section II presents the mathematical formulation of the problem. The description of the experiment setup and results are shown and discussed in Section III. Finally, the conclusion is presented in Section IV.

II. MATHEMATICAL FORMULATION

The physical interest problem is constituted of a real resonant cavity considering small losses where the surface currents are essentially those associated with the loss-free field solutions. This cavity is formed by a surface S_0 inclosing a volume V_0. It is considered, as an hypothesis, the volume of the perturbing object as being ΔV and the surface enclosing the perturbing object as being ΔS. The positive direction of ΔS is the outward direction of the volume ΔV. Here, the volume of the perturbed cavity is V and the surface enclosing it is S. Consider that the positive direction of S and S_0 is the outward direction of the cavity volume V and V_0. Besides, it is considered $S = S_0 - \Delta S$ and $V = V_0 - \Delta V$. Let ω_0, $\vec{E}_0$ and $\vec{H}_0$ represent the natural angular frequency, the electric and magnetic fields of the unperturbed cavity, respectively, and ω, $\vec{E}$ and $\vec{H}$ represent the corresponding quantities of the perturbed cavity. In both cases Maxwell's equations must be satisfied, that is

$$\nabla \times \begin{Bmatrix} \vec{E} \\ \vec{E}_0 \end{Bmatrix} = -j\mu_0 \begin{Bmatrix} \omega\vec{H} \\ \omega_0\vec{H}_0 \end{Bmatrix}, \tag{1}$$

This work was supported, in part, by FINEP (Research and Projects Financing) under contract 01.10.0430.00.

$$\nabla\times\begin{Bmatrix}\vec{H}\\ \vec{H}_0\end{Bmatrix}=j\varepsilon_0\begin{Bmatrix}\omega\vec{E}\\ \omega_0\vec{E}_0\end{Bmatrix}, \text{ and} \tag{2}$$

where ε_0 is the electric permittivity of free space and μ_0 is the magnetic permeability of the free space. The Maxwell's equations (1)-(2), conveniently manipulated [5] [6], result in the exact equation for the change in natural frequency due to the introduction of a conductive perturbing object into the cavity. Initially, one must multiply the complex conjugate of the second equation of (1) by $\vec{H}$, the first equation of (2) by $\vec{E}_0^*$, the complex conjugate of the second equation of (2) by $\vec{E}$ and the first equation of (1) by $\vec{H}_0^*$, obtaining

$$\vec{H}\cdot\nabla\times\vec{E}_0^* = j\omega_0\mu_0\vec{H}\cdot\vec{H}_0^*, \tag{3}$$

$$\vec{E}_0^*\cdot\nabla\times\vec{H} = j\omega\varepsilon_0\vec{E}_0^*\cdot\vec{E}, \tag{4}$$

$$\vec{E}\cdot\nabla\times\vec{H}_0^* = -j\omega_0\varepsilon_0\vec{E}\cdot\vec{E}^*, \text{ and} \tag{5}$$

$$\vec{H}_0^*\cdot\nabla\times\vec{E} = -j\omega\mu_0\vec{H}_0^*\cdot\vec{H}. \tag{6}$$

Then, subtracting (4) from (3) and (6) from (5) and using the vector identity given by

$$\nabla\cdot\left(\vec{A}\times\vec{B}\right)=\left(\nabla\times\vec{A}\right)\cdot\vec{B}-\left(\nabla\times\vec{B}\right)\cdot\vec{A}, \tag{7}$$

it is possible to write

$$\nabla\cdot\left(\vec{E}_0^*\times\vec{H}\right)=j\omega_0\mu_0\vec{H}\cdot\vec{H}_0^*-j\omega\varepsilon_0\vec{E}_0^*\cdot\vec{E}, \text{ and} \tag{8}$$

$$\nabla\cdot\left(\vec{E}\times\vec{H}_0^*\right)=j\omega_0\varepsilon_0\vec{E}\cdot\vec{E}^*-j\omega\mu_0\vec{H}_0^*\cdot\vec{H}. \tag{9}$$

The next step is to add (8) and (9), integrate over the volume V, and use the divergence theorem to obtain

$$\oint_S\left(\vec{E}\times\vec{H}_0^*+\vec{E}_0^*\times\vec{H}\right)\cdot d\vec{s}=-j\left(\omega-\omega_0\right)\int_V(\varepsilon_0\vec{E}\cdot\vec{E}_0^*+\mu_0\vec{H}\cdot\vec{H}_0^*)dv. \tag{10}$$

Now, since $\hat{n}\times\vec{E}=\vec{0}$ on S, expression (10) means that

$$\oint_S\vec{E}_0^*\times\vec{H}\cdot d\vec{s}=-j\left(\omega-\omega_0\right)\int_V(\varepsilon_0\vec{E}\cdot\vec{E}_0^*+\mu_0\vec{H}\cdot\vec{H}_0^*)dv. \tag{11}$$

In addition, since $S=S_0-\Delta S$ and $\hat{n}\times\vec{E}_0=0$ on S_0, it is possible to write that

$$\oint_S\vec{E}_0^*\times\vec{H}\cdot d\vec{s}=\oint_{S_0}\vec{E}_0^*\times\vec{H}\cdot d\vec{s}-\oint_{\Delta S}\vec{E}_0^*\times\vec{H}\cdot d\vec{s}=-\oint_{\Delta S}\vec{E}_0^*\times\vec{H}\cdot d\vec{s}, \tag{12}$$

Finally, using (14) in (13) one gets to

$$\Delta\omega=\omega-\omega_0=\frac{-j\oint_{\Delta S}\vec{E}_0^*\times\vec{H}\cdot d\vec{s}}{\int_V(\varepsilon_0\vec{E}\cdot\vec{E}_0^*+\mu_0\vec{H}\cdot\vec{H}_0^*)dv}. \tag{13}$$

For practical application of (13) and once that $\vec{E}$, $\vec{H}$, or ω are not generally known, it must replace these unknown perturbed quantities by the unperturbed fields $\vec{E}_0$ and $\vec{H}_0$, besides ω_0. For small perturbations, when ΔS is small, this is certainly reasonable and the denominator results

$$\int_V(\varepsilon_0\vec{E}\cdot\vec{E}_0^*+\mu_0\vec{H}\cdot\vec{H}_0^*)dv\approx\int_V(\varepsilon_0E_0^2+\mu_0H_0^2)dv. \tag{14}$$

In the numerator, the tangential component of the perturbed magnetic field is, approximately, equal to the unperturbed value when the conductive perturbing object is small. Then, it is possible to write that

$$\oint_{\Delta S}\vec{E}_0^*\times\vec{H}\cdot d\vec{s}\approx\oint_{\Delta S}\vec{E}_0^*\times\vec{H}_0\cdot d\vec{s}=\int_{\Delta V}\nabla\cdot\left(\vec{E}_0^*\times\vec{H}_0\right)dv. \tag{15}$$

Equation (15) can be written any other way. First, one must multiply the complex conjugate of the second equation of (1) by $\vec{H}_0$, and the second equation of (2) by $\vec{E}_0^*$, obtaining

$$\vec{H}_0\cdot\nabla\times\vec{E}_0^*=j\omega_0\mu_0H_0^2, \text{ and} \tag{16}$$

$$\vec{E}_0^*\cdot\nabla\times\vec{H}_0=j\omega_0\varepsilon_0E_0^2. \tag{17}$$

Then, subtracting (17) from (16) and using the vector identity (7) it is possible to write that

$$\nabla\cdot\left(\vec{E}_0^*\times\vec{H}_0\right)=j\omega_0\mu_0H_0^2-j\omega_0\varepsilon_0E_0^2. \tag{18}$$

Therefore, (15) can be rewritten as

$$\int_{\Delta V}\nabla\cdot\left(\vec{E}_0^*\times\vec{H}_0\right)dv=j\omega_0\int_{\Delta V}(\mu_0H_0^2-\varepsilon_0E_0^2)dv. \tag{19}$$

Substituting (14) and (19) into (13), it obtains

$$\frac{\Delta\omega}{\omega_0}\approx\frac{\int_{\Delta V}(\mu_0H_0^2-\varepsilon_0E_0^2)dv}{\int_V(\varepsilon_0E_0^2+\mu_0H_0^2)dv}. \tag{20}$$

This is the perturbation equation for conductor perturbation of a cavity. It is verified that the denominator is proportional to the total energy stored in the cavity, whereas the terms in the numerator are proportional to the electric and magnetic energies removed by the perturbation. Then, (20) can be rewritten as

$$\frac{\Delta\omega}{\omega_0}\approx\frac{\Delta W_m-\Delta W_e}{2W}, \tag{21}$$

where W denotes the total energy stored in the original cavity, and ΔW_m and ΔW_e denote the time average magnetic energy and electric energy, respectively, originally stored in the small volume ΔV. The perturbation equation shows that the introduction of a conductive perturbing object into the cavity will raise the natural frequency if it is made at a point with large magnetic field (high W_m) and small electric field (low W_e), and will lower the natural frequency if it is made at a point with large electric field (high W_e) and small magnetic field (low W_m).

The perturbation formulae (20) or (21) are valid only when the introduction of the perturbing object does not influence the fields outside the perturbing body. Otherwise, the perturbation formula must be modified as follows

$$\frac{\Delta\omega}{\omega_0}=K\frac{\int_{\Delta V}\left(\mu_0H_0^2-\varepsilon_0E_0^2\right)dv}{\int_V\left(\varepsilon_0E_0^2+\mu_0H_0^2\right)dv}=K\frac{\Delta W_m-\Delta W_e}{2W}, \tag{22}$$

where K is a constant and depends upon the shape of the perturbing object and the orientation of it in the fields. This perturbation constant K may be obtained by means of experiment.

In terms of the resonant frequency f_0 and the perturbed frequency shift Δf due to application of the method of perturbation it is possible, from (22), to write that

$$\Delta f=\frac{Kf_0}{4W}\int_{\Delta V}(\mu_0H_0^2-\varepsilon_0E_0^2)dv, \tag{23}$$

for small perturbations and where $4W$ is due to the fact that

$$W=\frac{1}{2}\int_V\left(\varepsilon_0E_0^2+\mu_0H_0^2\right)dv. \tag{24}$$

In TM_{010} klystron cavities, only the electric field is present along the cavity axis. Besides, experimentally, it is used the concept of the Slater's perturbation theorem, which states that, considering a small perturbing object along the axis, the magnetic field can be negligible [7] and the perturbed frequency shift, from (24), can be written as

$$\frac{\Delta f}{f_0} = -\frac{K\varepsilon_0}{4W}\int_{\Delta V}\left[E_z\left(f_0,r,z\right)\right]^2 dv\,. \qquad (25)$$

The cavity R_{sh}/Q_0, a figure of merit relating the resonant structure with its ability in doing work on an electron beam, is defined as the ratio of the shunt impedance R_{sh} of the cavity, in case of klystron cavities, given by

$$R_{sh} = \frac{\left[\int_{axis}\vec{E}\cdot d\vec{l}\right]^2}{2P_L} = \frac{\left[\int_{-\infty}^{+\infty}E_z\left(f_0,0,z\right)dz\right]^2}{2P_L}, \qquad (26)$$

and the unloaded quality factor Q_0, given by

$$Q_0 = \frac{\omega_0 W}{P_L}, \qquad (27)$$

where P_L is the power loss on the cavity walls [8]. Combining (26) and (27), one has

$$\frac{R_{sh}}{Q_0} = \frac{\left[\int_{-\infty}^{+\infty}E_z\left(f_0,0,z\right)dz\right]^2}{2\omega_0 W}. \qquad (28)$$

Now, multiplying and dividing (28) by $\int_{\Delta V}\left[E_z\left(f_0,r,z\right)\right]^2 dv$ results

$$\frac{R_{sh}}{Q_0} = \frac{\int_{\Delta V}\left[E_z\left(f_0,r,z\right)\right]^2 dv}{2\omega_0 W}\,\frac{\left(\int_{-\infty}^{+\infty}E_z\left(f_0,0,z\right)dz\right)^2}{\int_{\Delta V}\left[E_z\left(f_0,r,z\right)\right]^2 dv}. \qquad (29)$$

Isolating the term $\int_{\Delta V}\left[E_z\left(f_0,r,z\right)\right]^2 dv \Big/ 2\omega_0 W$ in (25) and substituting in (29), it is possible to write that

$$\frac{R_{sh}}{Q_0} = -\frac{\Delta f}{K\pi\varepsilon_0 f_0^2}\,\frac{\left(\int_{axis}E_z\left(f_0,b,z\right)dz\right)^2}{\int_{\Delta V}\left[E_z\left(f_0,r,z\right)\right]^2 dv}. \qquad (30)$$

The calculation of K is presented as the first result of the experiment in the next section. The integral ratio is obtained, experimentally, using the Slater's perturbation theorem.

III. Experiment and Results

First of all, it is necessary to calculate K. For this, it is used a cylindrical cavity (pill-box) and a metallic perturbing cylinder as shown in the Fig. 1. Table I presents their dimensions.

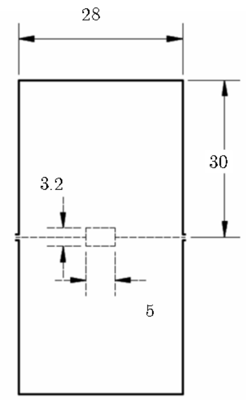

Fig. 1. Geometry and dimensions of the cylindrical cavity (pill-box) and perturbing object used in the perturbation method. The dimensions are in mm.

TABLE I. Dimensions of the cylindrical cavity (pill-box) and the metallic perturbing cylinder.

Quantity	***Value***
Cylindrical cavity length L, mm	28
Cylindrical cavity radius r_c, mm	30
Metallic perturbing cylinder length L_p, mm	5.00
Metallic perturbing cylinder radius r_p, mm	1.60
Volume of the perturbing object ΔV, mm^3	40.21

If the perturbing object is placed along the axis of pill-box in the TM_{010} mode, R_{sh}/Q_0 can be theoretically determined [8] [9] by

$$\frac{R_{sh}}{Q_0} = 185\frac{L}{r_c} = -\frac{L^2\Delta f}{K\pi\varepsilon_0\Delta V f_0^2}, \qquad (31)$$

where the gap factor reduces to 1.0 because the electric field in a TM_{010} cylindrical cavity is constant across L. Thus, K becomes

$$K = -\frac{r_c L\Delta f}{185\pi\varepsilon_0\Delta V f_0^2}. \qquad (32)$$

A metallic perturbing cylinder, shown in Fig. 2, was calibrated in this way using the cylindrical cavity shown in Fig. 1.

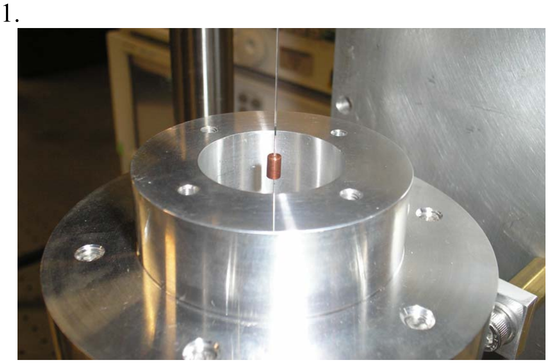

Fig. 2. Metallic perturbing cylinder used in the perturbation method.

The perturbation measurements starting point is the calibration of a port of the Agilent PNA N5230C Network Analyser used in the experiment. Next, the calibrated port of the network is connected to the coupling probe in the cavity, one should select the parameter S_{11} or S_{22} to find out the frequency f_0 without the perturbing object. Thereafter, the experiment is repeated with the metallic perturbing cylinder placed along the axis of a cavity and the perturbed frequency shift Δf is recorded. Substituting the experimental values of f_0 and Δf in (32), besides the dimensions shown in Table I, one can find the value of *K*, presented in Table II. Moreover, a 3D eigensolver was used to simulate the cavity for comparison purposes.

TABLE II. RESULTS OF THE PERTURBATION METHOD APPLIED TO CALCULATE THE CAVITY R_{sh}/Q AND COMPARISON WITH THE QUANTITIES CALCULATED BY THE 3D EIGENSOLVER. IT WAS USED THE CYLINDRICAL CAVITY (PILL-BOX) SHOWN IN FIG. 2.

Quantity	***Values***	
	Experiment	***3D eigensolver***
Frequency f_0, GHz	3.82551	3.82443
Perturbed frequency shift Δf, MHz	–19.80	–21.42
Perturbation constant K	5.57	5.95

The next step is, using the klystron cavity built in the laboratory with dimensions as in Fig. 3 and the metallic perturbing cylinder, showed in the Fig. 2, to determine the R_{sh}/Q_0 using the perturbation method. The reentrant cavity geometry is shown in Fig. 4.

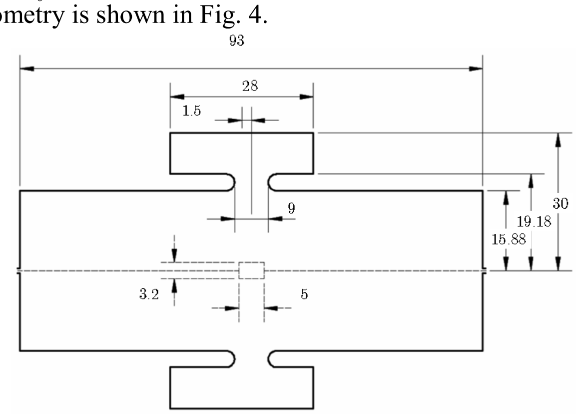

Fig. 3. Geometry and dimensions of the reentrant cavity used in the perturbation method. The dimensions are in mm.

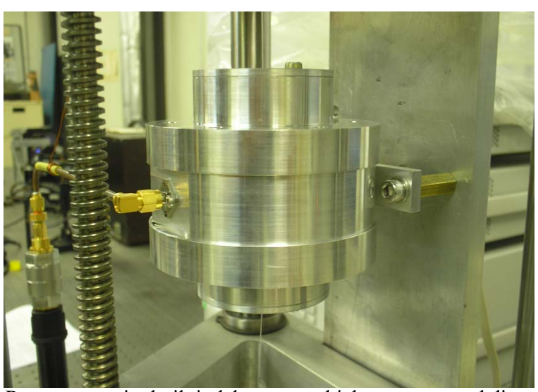

Fig. 4. Reentrant cavity built in laboratory which geometry and dimensions are presented in Fig.3.

The experimental setup is shown in Fig. 5. Initially, two copper foils of 0.2 mm thickness each were placed between the cavity body and the openings of the cavity, to act as electromagnetic chokes, in order to stop the electromagnetic leakage from the cavity. Then, following the same steps described before, the first determination is the frequency f_0 without the perturbing object. Actually, the perturbing object is kept all the time inside the cavity axis but, for this first measurement, its position is far enough from the center and, since the electric field is evanescent, it is considered that the field is negligible and the perturbing object does not affect the measurement.

Fig. 5. Experimental apparatus used in the calculation of the cavity R_{sh}/Q_0 using the perturbation method.

Afterwards, the experiment is repeated with the metallic perturbing cylinder placed along the axis at the position where the perturbed frequency shift Δf is a maximum. This deviation can be seen in Fig. 6, which is the PNA display.

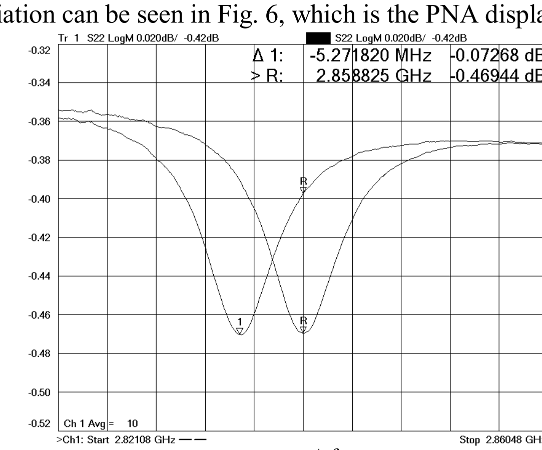

Fig. 6. The perturbed frequency shift Δf calculated by the perturbation method.

Furthermore, it is possible, using the concept of the Slater's perturbation theorem and the experiment, to plot the graph of the axial electric field along the cavity axis. The result is compared with the profile of the axial electric field in a cavity with offset gap considering a hyperbolic profile, according to the development presented in [9] and where the gap of interaction is symmetric with respect to the position z_g and the electric field in the gap region is considered as a combination of two functions: for $z < z_g$ the electric field in the interaction gap has a hyperbolic profile given by $E_M \cosh(q_1 z)$, otherwise it has a hyperbolic profile given by $E_M \cosh(q_2 z)$, where E_M is the electric field amplitude, q_1 and q_2 are constants. Considering b as the drift tube radius, Fig. 7 shows the distribution of electric field in the axial coordinate of the gap ($r = b$) and for some values inside the drift tube. It is possible to observe that it is an evanescent field.

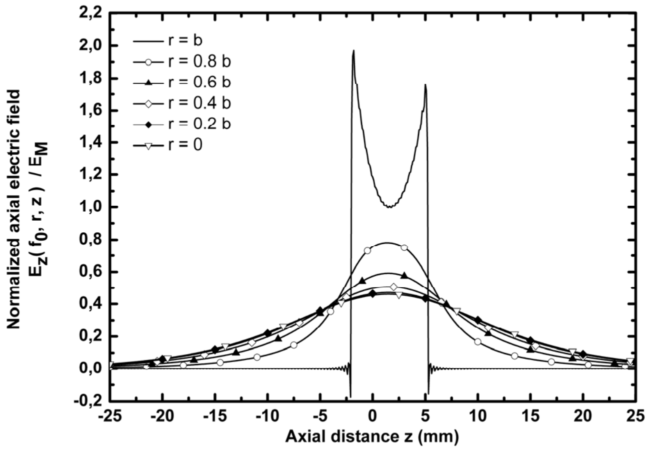

Fig. 7. Distribution of electric field in the axial coordinate of the gap ($r = b$) and for some values inside the drift tube, considering the hyperbolic profile. It is observed that this field is evanescent [9].

The same result can also be obtained by simulating a klystron cavity using a 3D eigensolver. Fig. 8 shows the three results for $r = 0$.

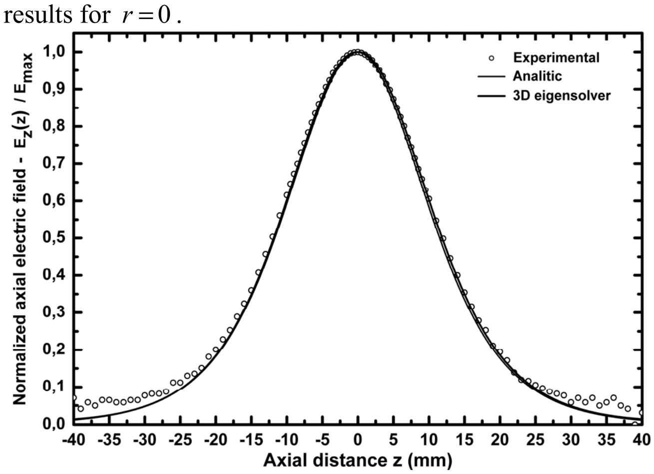

Fig. 8. Normalized axial electric field calculated experimentally and using, for comparison purposes, the 3D eigensolver and the analytic expression presented in [9].

Substituting the experimental values of f_0 , Δf and K in (30), besides the value of the integral ration obtained from the experimental results of the electric field shown in Fig. 8, one can find the value of cavity R_{sh} / Q_0 , which is presented in Table III, together with the value calculated using the analytic expressions and the simulated result from the 3D eigensolver, both used for comparison purposes.

TABLE III. RESULTS OF THE PERTURBATION METHOD APPLIED TO CALCULATE THE CAVITY R_{sh} / Q_0 AND COMPARISON WITH THE QUANTITIES CALCULATED USING THE ANALYTIC EXPRESSIONS AND THE 3D EIGENSOLVER. IT WAS USED THE REENTRANT CAVITY SHOWN IN FIG. 4.

Quantity	***Values***		
	Experiment	***Analytic***	***3D eigensolver***
Frequency f_0 , GHz	2.859	2.875	2.872
Perturbed frequency shift Δf , MHz	−5.27	−5.27	−5.90
Perturbation constant K	5.57	5.57	-----
Cavity R_{sh} / Q_0 , Ω	79.8	74.9	79.7

The deviation between the experimental and the analytic value is around 6 % while the experimental and simulated value is less than 0.5 %, which demonstrates that the experimental procedure presented is very effective in measuring R_{sh} / Q_0 .

It is interesting to observe the negative signal of the perturbed frequency shift Δf , which indicates that the presence of the perturbing object decreased the natural frequency. This phenomenon occurs when the perturbing object is put in a position with large electric field (high W_e) and small magnetic field (low W_m). This is exactly the case, confirmed by calculating the integral ratio using the analytic expressions without neglecting the magnetic field (23). It was obtained for cavity R_{sh} / Q_0 the value of 75.0 Ω , less than 0.14 % . This result is interesting because it indicates that the calculation using only the electric field (magnetic field is negligible) is sufficient to have a good accuracy.

IV. CONCLUSION

In this work the results of a klystron cavity R_{sh} / Q_0 using the perturbation measurements was presented. The R_{sh} / Q_0 expression involves the natural frequency f_0 , the perturbed frequency shift Δf , the perturbing constant K and the axis factor which relates the electric field along the cavity axis and the electric field in the volume of the perturbed object. The two first parameters were measured using a cylindrical reentrant cavity with offset gap built in the laboratory: f_0 using an unperturbed cavity and Δf using the same cavity perturbed by a metallic perturbing cylinder. The perturbing constant K was calculated by measuring the same parameters mentioned above using a cylindrical cavity (pill-box). The integral ratio was obtained experimentally using the Slater's perturbation theorem. It was verified a good agreement between the cavity R_{sh} / Q_0 obtained by the experiment and the values found with the analytic expressions and the 3D eigensolver as well.

REFERENCES

[1] G. Goplen, L. Ludeking, D. Smithe, and G. warren, "User-configurable MAGIC for electromagnetic PIC simulations", *Comput. Phys. Commun.*, vol. 87, pp. 54-86, 1995.

[2] K. Halbach and R. F. Holsinger, "SUPERFISH -- A Computer Program for Evaluation of RF Cavities with Cylindrical Symmetry," Particle Accelerators 7 (4), 213-222 (1976).

[3] CST, Computer Simulation Tecnology. CST STUDIO SUITE^{TM} 2008 getting started. 2008.

[4] J. C. Slater, Microwave Electronics. New York, N.Y.: Dover Publications, 1950.

[5] D. M. Pozar, Microwave Enginnering. New York, USA: Addison-Wesley Company Inc, 1993.

[6] K. Zhang, D. Lee, Electromagnetic Theory for Microwaves and Optoelectronics. 2nd ed. Leipzig, Germany: Springer, 2008.

[7] D. J. Liska, "Electric field measurements in klystron cavities," *IEEE Transactions on Electron Devices.*, vol. 18, no. 7, pp. 450- 453, jul. 1971.

[8] R. J. Barker, J. H. Booske, N. C. Luhmann Jr., G. S. Nusinovich, Modern Microwave and Millimeter-wave Power Electronics. 2nd ed. New Jersey, N.J.: John Wiley & Sons, 2005.

[9] R. K. Silva, D. T. Lopes and C. C. Motta, "Analytical determination of lumped parameters of reentrant klystron cavities," *IEEE Transactions on Electron Devices*, to be published.